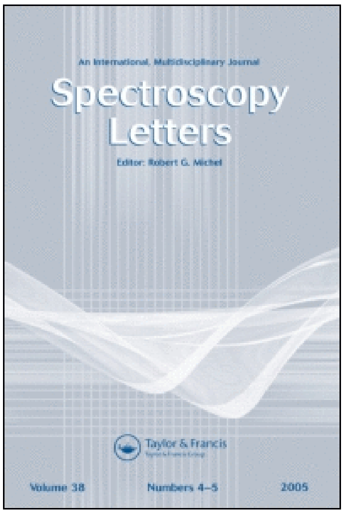

Spectroscopy Letters
Publication details, including instructions for authors and subscription information:
http://www.informaworld.com/smpp/title~content=t713597299

Palladium Release in Electrothermal Atomic Absorption Spectrometry

Vera I. Slaveykova[a]; Stefan G. Manev[a]; Dobri L. Lazarov[a]
[a] Faculty of Chemistry, University of Sofia, Sofia, Bulgaria

To cite this Article Slaveykova, Vera I. , Manev, Stefan G. and Lazarov, Dobri L.(1997) 'Palladium Release in Electrothermal Atomic Absorption Spectrometry', Spectroscopy Letters, 30: 2, 297 — 307

To link to this Article: DOI: 10.1080/00387019708006989

URL: http://dx.doi.org/10.1080/00387019708006989

SPECTROSCOPY LETTERS, 30(2), 297-307 (1997)

PALLADIUM RELEASE IN ELECTROTHERMAL ATOMIC ABSORPTION SPECTROMETRY

Key words: ETAAS, Atomization, Palladium Release, Kelvin Equation , "Effective" Radius.

Vera I. Slaveykova*, Stefan G. Manev, Dobri L. Lazarov
Faculty of Chemistry, University of Sofia, 1 James Bourcier, Sofia 1126, Bulgaria

ABSTRACT

The absorbance signal in electrothermal atomic absorption spectrometry is a result of the processes of atom formation and dissipation and first of all depends on the initial generation of atoms from the surface. The rising part of the absorbance time profiles can be used for characterization of the release of the metals like Pd, Ag, Au etc. The method is applied to investigate the palladium release from a pyrocoated graphite support at different initial masses of the Pd. The kinetic parameters are evaluated and conclusions about the distribution of palladium on the graphite surface are made. The estimated values of apparent activation energies depend on the initial mass of analyte. The advantages and limitations of the present approach are discussed.

---

* Corresponding author; Fax: ++3592 9625438

E-mail: slaveikova@chem.uni-sofia.bg

INTRODUCTION

Along with the wide application of electrothermal atomic absorption spectrometry (ETAAS) as a powerful method for trace analysis, it is of fundamental interest to study its possibilities as a tool for investigation of the desorption and vaporization of the metals from the graphite support.

Recently the efforts of the scientist in the area of atomic absorption spectrometry were oriented to study atomization mechanisms. The various kinetic models describing atom formation were proposed [1-3] and lately precised [4-8].

The aim of the present work is to demonstrate the potential of ETAAS as a method for investigation of the vaporization and flash desorption of the metal atoms from the graphite support and to use absorbance signal for assessment of the kinetic parameters.

The method is applied to the example of the palladium release, because of both its important roles as a catalyst in various industrial processes and effective and wide application in ETAAS as a chemical modifier [9].

The processes of atom formation of Pd in graphite atomizer were investigated [10] and it was found that the processes were described by a first order equation and activation energy 175 kJ/mol, the value independent of the analyte mass.

By means of scanning electron microscopy (SEM) the existence of Pd microdroplets on the graphite at μg amounts [11,12] was shown. Well separate particles with an approximate diameter 0.1 μm were observed by SEM using 300 ng of Pd after thermal treatment at 1100°C [13]. The high disperse distribution of the sample on the graphite after an aerosol sample deposition for ng amounts of palladium were reported [14].

This approach is expected to provide an information on the pattern of metal distribution on the graphite surface as well as on the interface interaction and transitions related to interpretation of the experimentally evaluated activation energy.

EXPERIMENTAL

In the present study the amounts of Pd is varied within a wide range, including vaporization from ng amounts of Pd as analyzed in ETAAS to μg amounts of Pd as common for the chemical modifiers [9].

Sample layer preparation

Aliquots of ten μl of the solution of $Pd(NO_3)_2$ and a reducing agent are injected automatically between internal rings of the "partitioned" graphite tubes by means of autosampler syringe. The working solutions containing 30, 60, 90, 120, 210, 420 μg/l for ng level and 6, 30, 60, 90, 120 mg/l for μg level experiments were prepared daily after appropriate dilution of the stock standard (0.6% m/V $Pd(NO_3)_2$) in double distilled water. The volume of the injected samples, hence the area occupied of the sample solution droplet are the same for various concentration. Therefore, a proportionality between the initial mass of the sample and surface coverage could be assumed.As a reducing agent hydroxylamine hydrochloride is used to insure earlier transformation of the palladium salt to the metal.

Thermal treatment of the sample

Thermal treatment of the sample includes consecutive stepwise heating at 120°C temperature (10s ramp and 10s hold times) during drying, 300°C (10+10), 900°C (1+10) pyrolysis, 300°C (5+1) cool down, 2400°C (1+3) atomization and 2600 °C for 2 s for clean up of the tube .

Absorbance signal measurement

The dependence of the absorbance and temperature of the tube vs time, the peak height and peak area are recorded. The additional temperature control of the tube heating is realized by optical pyrometer focused on the bottom of the tube through the injection port. So obtained signal is used for further calculations

The experiments were carried out on Varian SpectrAA 400 Zeeman spectrometer, equipped with a GTA 96 graphite tube atomizer and programmable sampler dispenser. Argon is used as a purge gas. The instrument parameters are as follows: wavelength 244.8 nm, bandpass 0.2 nm and gas stop during atomization for the ng series of experiments and wavelength 340.5 nm, bandpass 1.0 nm and gas flow during atomization for the μg series of experiments. The availability of several wavelengths with different sensitivity facilitates measurements and extends the working interval of the concentrations and also determines the choice of Pd as an analyte. There is a proportionality between the mass of the sample and the absorbance signal for both series under conditions employed.

Kinetic analysis of data

For kinetic analysis of experimental data, the Coats and Redfern approach, describing the processes at the conditions of linear increase of the temperature, was applied [18]. The equation used for evaluation of the activation energy of the release process is:

$$\ln [g(a).T^{-2}] = - E_a.(R.T)^{-1} + \ln[A.R.P.(RH.E_a)^{-1}] \quad (1)$$

where :

g(a) is a function depending on the rate limiting process; a is a factor of conversion, which in the present case is equal to A_t/A_{max} [19]; RH is the heating rate; A is the frequency factor; $P=1-2x+6x^2-24x^3+120x^4....$; $x=RT/E_a$; T is the absolute temperature; R is the universal gas constant; A_t is the measure absorbance at time t; A_{max} is the maximum absorbance.

RESULTS AND DISCUSSION

An example of absorbance vs time profiles experimentally observed at various initial amounts of Pd are presented on Figs. 1 a and b for ng and μg levels, respectively. As the initial amounts of Pd increased, there is a shift to an earlier appearance times (temperatures) but peak maximum times remain nearly constant at ng Pd levels. These features might indicate a first order process [15].

At μg levels, the times corresponding to the maximum absorbance are enhanced with increasing the initial amount of Pd and the peaks are relatively sharp and narrow, which according to Mc Nally and Holcombe [15], indicate a fractional order of release.

Since the shape and position of the absorbance-time profiles depend on various factors such as the heating rate, temperatures and times of thermal pretreatment and atomization [16,17], the experiments are carried out at identical conditions.

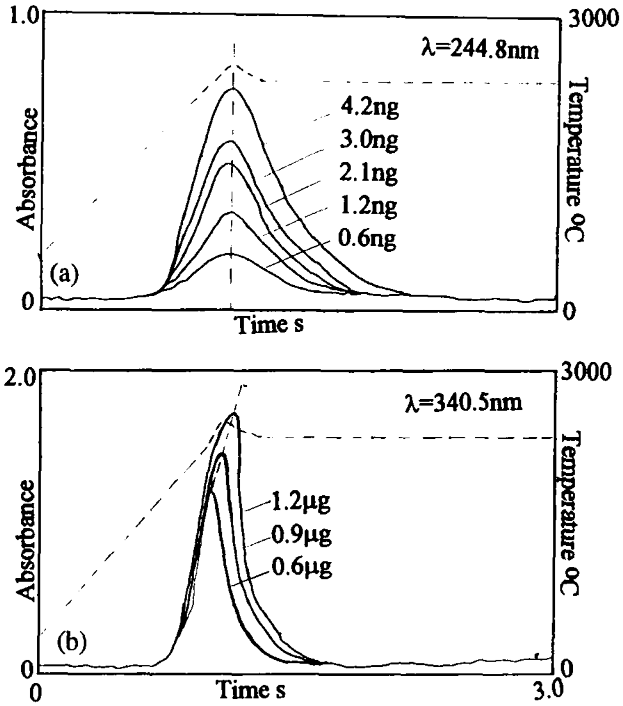

Fig. 1. Examples for the absorbance-time profiles for (a) ng and (b) μg amounts of Pd.

On the basis of the dependence of absorbance profiles on the initial mass/surface coverage discussed above the expressions $-\ln(1-a)$ for $n=1$; $[1-(1-a)^{1/2}]$ for $n=1/2$ and $[1-(1-a)^{1/3}]$ for $n=1/3$ are used for function g(a). The activation energy of the release is evaluated from the slope of the linear "Arrhenius" plot $\ln[g(a).T^{-2}]$ vs $1/T$.

The examples for "Arrenius" plots are shown on the Fig. 2 for 0.9 ng, 3.0 ng and 1.2 μg initial masses of Pd.

As could be expected, the best possible fit between experimental data and theoretical equations is observed for n=1 at ng levels of Pd. The experimental data for μg levels are described with the same accuracy from the function g(a) at n=1/2 and 1/3 and the estimated

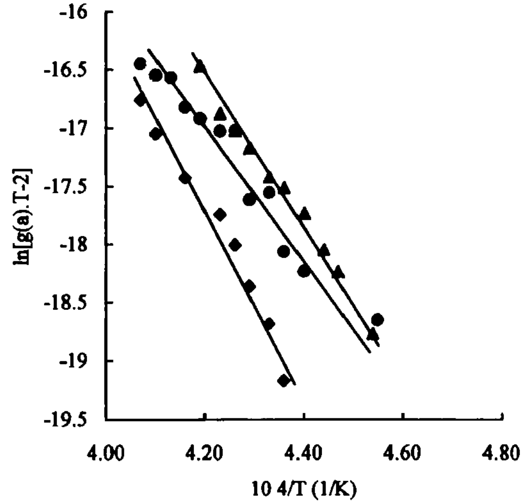

Fig. 2. Arrenius plots for (•) 0.9 ng, (Δ)3.0 ng and (♦)1.2 μg palladium.

values of E_a are close. The obtained activation energies are summarized in the Tables 1 and 2 for ng and μg levels of Pd, respectively.

Let us consider the ng level set of experiments, as the initial amount / surface coverage increased, the activation energy increases and achieves 591± 31 kJ/mol at 4.2 ng Pd, value, close to those for μg set experiments.

A similar tendency was observed for silver and gold [16] and successfully explained by applying the Kelvin equation [8]. It was shown that the estimated activation energies E_a are equal to the enthalpy of vaporization ΔH_r of silver and gold droplets with "effective" radius r. The changes in activation energies E_a follow the increase of ΔH_r with radius of the particles and for the sufficiently large particles the E_a approaches to the enthalpy of vaporization from the plane surface ΔH_v. Likewise, the activation energy for sufficiently large amounts of Pd approaches a constant value. In contrast to Ag, where $E_a = \Delta H_v$, the values of activation energies for palladium release are higher than the

Table 1. Actvation energies E_a at various initial mass, n=1, ng levels (mean of 4 experiments ± standard deviation).

Initial mass in ng	0.6	0.9	1.2	2.1	3.0	4.2
E_a kJ/mol	354 ±12	418 ±18	481± 13	513 ±16	545± 21	591±31

Table 2. Activation energies E_a at a various initial mass of Pd at μg levels (mean of 4 experiments ± standard deviation).

Initial mass in μg	0.3	0.6	0.9	1.2
E_a kJ/mol ; n=1/2	585±19	571±23	571±18	626±23
E_a kJ/mol ; n=1/3	562±23	558±18	559±17	606±21

enthalpy of vaporization of Pd from a plane surface. Therefore, it could be assumed that the estimated values of E_a include not only ΔH_r , but also other parameters related to interaction between Pd and graphite support. For example, activation energy of desorption E_d , which summarized the enthalpy of adsorption and the activation energy of adsorption (if adsorption is activated) might reflect the interaction with graphite support at ng levels. The values of E_d and ΔH_r are mass dependent as E_d decreases and ΔH_r increases with increasing the initial mass/surface coverage. Moreover, the interaction with the support leading to deformation of the droplets at μg level could be characterized by a cohezive energy.

Using the already known relation between the initial mass of sample and the "effective" radius of particles [8] and assuming the Kelvin equation being valid, it is possible to estimate the activation energy of desorption, E_d . The SEM data of Docekalova et al.[13] giving an approximate radius 5.10^{-8}m of the particle for 300ng of palladium also are taken into account.

The theoretical dependence of ΔH_r on the reciprocal radius of the particles and experimentally observed E_a values vs 1/r are shown on Fig 3.

The intercept of the $\Delta H_r = f(1/r)$ plot is ΔH_v and slope is related to the shape of the particles and received at higher temperature droplets. In the "ideal" case there is no interaction between droplets and graphite support and the resulting droplets are spherical.

The dependence of the experimental activation energy E_a vs reciprocal radius 1/r is also linear. The intercept can be a sum of the enthalpy of vaporization from the plane surface ΔH_v and activation energy of desorption E_d and the slope is about two times smaller than the "ideal" one. That is not unexpected, taking into account the dependence of the slope on the surface tension, which decreases with increasing of the interaction of the palladium with graphite [8].

Thus, considering the dependences of ΔH_r and E_a on 1/r could be possible to evaluate the values of the activation energy of desorption for the different initial mass of the analytes.

As can be seen with increase of the initial coverage the E_d increases and plays the prevailing role at a very low coverage. For example at 0.6 ng, the atom release of Pd is determined exceptionally by E_d and the "effective" radius of the particles is of the same order as atomic radius for Pd. At sufficiently higher particles $\Delta H_r \rightarrow \Delta H_v$ and $E_d \rightarrow 136$ kJ/mol, which corresponds to the initial mass of 4.2 ng.

Let us recall that the "effective" radius is a mean value and is determinated on tha basis of a Kelvin equation. In fact it might be far from the real size of the particles on the graphite.

Therefore, it is possible that palladium is distributed as a high dispersed atoms or clusters with dimensions about 5-10 atomic radii of Pd [20] and is characterized with strong palladium graphite interaction at the small initial coverages. This is confirmed by dependence of the absorbance profiles on the initial masses (see Fig. 2a) and high resolution transmission electron microscopy study of Yosuda el al. , which observed Pd clusters with 2 to 5 nm diameter [21]. It is also in consistence with investigations of Holcombe and McNally [15]. Using the time and spatial resolved absorbance profile studies they depicted

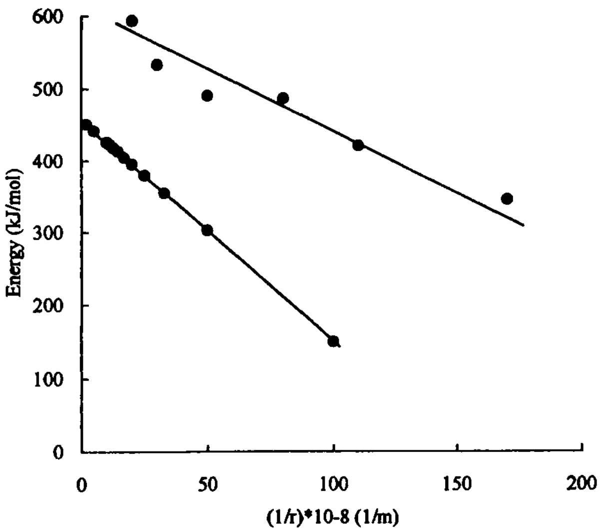

Fig. 3. Theoretical dependance of ΔH_r at 2173 K (a) and experimental values of E_a as a function of the reciprocal value of the effective radius (b).

the appearance of atomic gradient from the bottom to the furnace top during the rising portion of the peak, which point to relatively strong palladium graphite interaction [15].

The obtained values of E_a are mass independent, a cohezive energy approaches to about 130kJ/mol, $\Delta H_r \rightarrow \Delta H_v$ and "effective" radius of the particles is >5×10^{-8}m at µg amount Pd. Furthermore, the existence of Pd microdroplets on the graphite can be concluded. The fractional order of release and investigations with SEM [11] also point to the existence of Pd microdroplets on the pyrocoated graphite support.

The present consideration could be supported by simple theoretical calculations. Thus, the rough theoretical estimation indicates, that 4.6×10^{14} atoms Pd are required to cover 2×10^{-5} cm^2 area as a monolayer. Moreover, the number of particles, which correspond to 0.6ng and 1.2µg Pd - boundary masses in our study are 3.4×10^{12} and

7×10^{15} atoms respectively. Hence, the high disperse spatial distribution at ng level samples and agglomeration at high levels could be expected.

CONCLUSION

Electrothemal atomic absorption spectrometry is applied to investigate the vaporization of palladium from pyrocoated graphite support in the conditions of fast temperature increase up to 1500K/s. The absorbance signal, obtained during atomization of various masses of Pd is used for estimation of kinetic parameters - order of release, activation energy of atomization and activation energy of desorption. Palladium desorbs as individual atoms, which indicates relatively strong palladium graphite interaction and results in an apparent first order release at an initial mass up to 4.2 ng. The estimated activation energies increase with increasing of the initial mass.

For μg levels of palladium the estimated values of activation energy are independent of the initial mass and absorbance time profiles indicate on fractional order of release and an existence of microdroplets on the graphite.

REFERENCES

1. R. Sturgeon, C. Chakrabarti and C. Langford, *Anal. Chem.* **48** (1976) 1792.

2. B. Smets, *Spectrochim. Acta Part B* **35** (1980), 33.

3. C. Chung, *Anal. Chem.* **56** (1984) 2714.

4. C. Chakrabarti and S. Cathum, *Talanta* **38** (1991) 157.

5. Yan Xin-ping, Ni Zhe-ming, Yang Xiao-tao and Hong Guo-qiang, *Spectrochim. Acta Part B* **48** (1993) 605.

6. D. Rojas and W. Olivares, *Spectrochim. Acta Part B* **47** (1992) 387.

7. R. Fonseka, L. Pfeferkorn and J. Holcombe, *Spectrochim. Acta Part B* **49** (1994) 1595.

8. V. Slaveykova, S. Manev and D. Lazarov, *Spectrochim. Acta Part B* **50** (1995).

9. D. Tsalev, V. Slaveykova and P. Mandjukov, *Spectrochim. Acta Rev.* **13** (1990) 225.

10. J. Mc Nally and J. Holcombe, *Anal. Chem.* **63** (1991) 1918.

11. L. Voth-Beach and D. Shrader, *J. Anal. At. Spectrom.* **2** (1987) 45.

12. T. Baird, J. Frier, A. Arbuthnott, B. Mc Aneney and E. Riddell, *Carbon* **12** (1974) 381.

13. H. Docekalova, B. Docekal, J. Komarek and I. Novotny, *J. Anal. At. Spectrom.* **6** (1991) 661.

14. S. Sachesenberg, T. Klenke, W. Krumbein, H. Schellnhuber and E. Leeck, *Anal. Chim. Acta* **241** (1993) 279.

15. J. Mc Nally and J. Holcombe, *Anal. Chem.* **59** (1987) 1105.

16. S. Lynch, R. Sturgeon, V. Luong and D. Littlejohn, *J. Anal. At. Spectrom.* **5** (1990) 311.

17. R. W. Fonseca, J. Mc Nally and J. Holcombe, *Spectrochim. Acta, Part B,* **46** (1994) 79.

18. A. Coats and J. Redfern, *Nature (London)* **201** (1964) 68.

19. S. Shojilmai and Y. Hayashi, *Bull. Chem. Soc. Jpn.* **65** (1992) 871.

20. L.N. Lewis, *Chem. Rev.* **93** (1993) 2693.

21. K. Yosuda, Y. Hirano, T. Kamino, T. Yaguchi and K. Hirokawa, *Anal. Sci.* **11**, (1995) 437.

Received: July 29, 1996
Accepted: October 5, 1996